Hydraulic conductivity changes and influencing factors in longwall overburden determined by slug tests in gob gas ventholes

C. Özgen Karacan *, Gerrit Goodman

National Institute for Occupational Safety and Health (NIOSH), Pittsburgh Research Laboratory, PO Box 18070, Pittsburgh, PA 15236, USA

A B S T R A C T

This study presents the results of core-log analyses from the exploration boreholes, the analyses of face advance rates, and the results of downhole monitoring studies performed in gob gas ventholes for calculation of changes in hydraulic properties in the longwall overburden at a mine site in southwestern (SW) Pennsylvania section of Northern Appalachian Basin. In the first part of the study, coal measure rocks in overburden strata were analyzed and the locations where possible fractures and bedding plane separations would occur were evaluated. In the second part, the hydraulic conductivities were computed by two different slug test analyses methods using the water level changes measured in gob gas ventholes as longwall face approached. Hydraulic conductivities were analyzed with respect to the changes in overburden depth, the locations of the borehole, and mine face advance rates. These data were used to interpret the potential productivities of the gob gas ventholes as a result of fracturing and changes in hydraulic conductivities.

The general results showed that the probability of fracturing and bedding plane separations in the overburden increase between strong and weak rock interfaces. Also, the probability of bedding plane separations increases as the interface is close to the extracted coal seam. Evaluation of slug tests showed that the hydraulic conductivity developments in the boreholes and their potential production performances are affected by the underground strata and the roof materials. In situations where the roof material is stiff and thick, the development of high permeability fractures around the borehole will be less. Results also indicated that borehole location with respect to face position affects the fracturing time and permeability evolution as well. Greater overburden depths generally cause earlier fracturing as longwall face approaches, but eventually result in lower hydraulic conductivities and potentially less effective boreholes. Increasing mining rates also resulted in generally lower hydraulic conductivities in the overburden. The results of this study were intended to improve the interpretation of gob gas venthole performance and to provide better siting of these boreholes.

1. Introduction

Methane inflow from overburden strata during longwall mining is affected by the magnitude of fracturing and the time that the fractures stay open as the panel is extracted. The reservoir characteristics and their changes during mining also affect production potential of the gob gas ventholes (GGVs) that are commonly used to control the methane emissions from the fractured zone and are drilled from the surface to a depth that places them above the caved zone [1]. This consequently impacts the efficiency of methane drainage and control in the mining environment. Thus, the ability to predict changes in formation characteristics based on various factors at a given location increases the understanding of GGV production and provides improved placement where they may be more productive.

Singh and Kendorski [2] and Kendorski [3] evaluated the disturbance of rock strata resulting from mining beneath surface water and waste impoundments. In their analysis, they describe a caved zone that extends from the mining level to 3–6 times the seam thickness, a fractured zone that extends from the mining level to 30–58 times the seam thickness, an aquiclude zone where there is no change in permeability that extends from 30 times the seam thickness to 50 ft below ground surface, and a surface cracking zone that is 50 ft thick (Fig. 1). Hasenfus [4] described the hydro-geomechanics of overburden aquifer response to longwall mining with specific relation to the Pittsburgh coal seam in West Virginia. Based on the measurements, the overburden was divided into four zones: a gob, a highly fractured zone, a composite beam zone and a surface layer. Palchik [5] reported that, based on the measurements in the Donetsk coal basin, the thickness of the

* Corresponding author. Tel.: +1 412 386 4008; fax: +1 412 386 6595.
E-mail address: cok6@cdc.gov (C. Özgen Karacan).

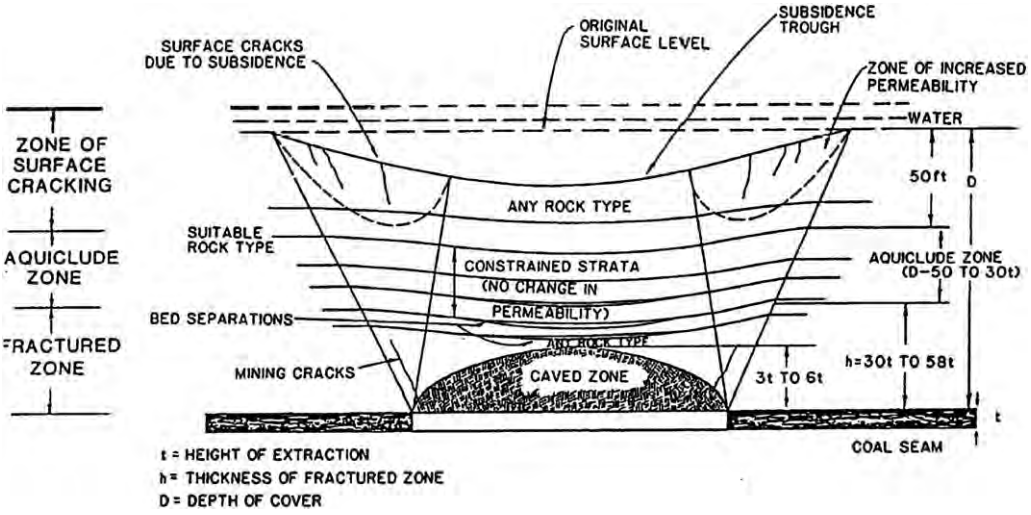

Fig. 1. Strata behavior of surface and subsurface zones as a result of longwall mining [2].

fractured zone can vary up to 100 times the height of the mined coal bed depending on the size of the panel and the geology and geomechanical properties of the layers.

The characteristics of fracturing and the subsidence of overburden are also revealed through predictive techniques and field studies. Li et al. [6] investigated the distribution of overburden fracturing, the distribution pattern of methane and methane migration mechanisms in the mining-induced fracture zones, and the subsidence over a longwall panel based on the results in a physical model. Cui et al. [7] performed a prediction study for the progressive surface subsidence above longwall mining using a time function. They calculated differential subsidence characteristics, such as progressive slope, progressive curvature and horizontal strain. Luo [8] predicted that the subsidence velocity distribution along the longwall face is a normal distribution with respect to the location of the on-going longwall face. Surface dynamic characteristics were also linked to the longwall advance rate. Preusse [9] discussed the surface time-dependent effects and their relations with the face advance rates. He suggested that regulating the advance rate in a longwall mining operation can be an effective means for reducing the potential disturbance to surface structures.

The change in hydraulic conductivity over and around longwall panels as a result of fracturing and subsidence, which is of primary importance for controlling methane from gobs using GGVs, was initially investigated for its potential effect on surface water resources [10]. A combined finite element model of the deformation of the overlying strata and its influence on ground water flow was used to define the change in local and regional water resources. Their results showed that there would be no predicted long term effects of longwall mining on ground water flow. Fawcett et al. [11] described a theoretical investigation into the zones of increased hydraulic conductivity caused by rock failure above a longwall panel. They correlated predicted failure heights with existing experimental values. Changes in the three-dimensional hydraulic conductivity field that accompany undermining by a longwall panel were evaluated by Liu and Elsworth [12] to define the potential for changes in flow patterns and desaturation. The model results showed that hydraulic conductivity increases were restricted to shallow depths ahead of the advancing face and to deep zones behind the face, particularly in the caving and abutment shear zones. Gale [13] used computer modeling techniques to simulate rock fracture, caving, stress redistribution, and induced hydraulic conductivity enhancements around longwall panels. As a result of this study, he reported that the horizontal conductivity can be significantly enhanced along bedding planes within and well outside the panel. This probably will vary depending on the nature of each site. Also, Whittles et al. [14,15] conducted studies on the effects of different geotechnical factors on gas sources and gas flow paths for UK longwall operations. They studied how roof geology and its interactions with boreholes may cause the deformation and closure of the boreholes drilled for methane control.

From a methane control point of view, hydrologic reservoir characteristics and their variations during mining affect both the emissions of gas into mine workings and the production potential of the GGVs that are used to mitigate these emissions [16]. Slug tests are widely used by hydrologists to evaluate hydraulic conductivities of aquifer horizons. Although they are frequently used to evaluate water conductivities of aquifers, soils and mine-waste areas created in surface mining [17–20], their use in longwall overburden is limited. The use of slug tests in active GGVs to measure the transient changes in hydraulic conductivities as a function of time and face location is currently non-existent in the literature. This paper presents an integrated study of evaluation of underground strata, their predicted potential responses to longwall mining, and evaluations of mining rate effects using "in-situ" slug tests. These tests were performed in GGVs to characterize the changes in hydraulic conductivities of the slotted sections of the boreholes.

2. General information on the geology and hydrology of coal fields in Southwestern (SW) Pennsylvania—study site

The vast majority of coal in Pennsylvania was deposited during the Pennsylvanian period [21]. The largest production of underground coal in Pennsylvania is mined from the Pittsburgh coal seam which is the base of the Monongahela Group. The Monongahela Group encompasses the stratigraphy from the base of the Pittsburgh coal bed to the base of the Waynesburg coal bed, extending to a thickness of 270–400 ft (82–122 m). In mining of the Pittsburgh coal bed, the source of methane was found to be mainly between the Sewickley coal bed horizon and the top of Pittsburgh coal bed. Thus, a specific emphasis was given in this study, as will be seen in the next sections, to the strata below the Uniontown sandstone, including the Sewickley limestone and coal bed.

Ground water movement in SW Pennsylvania section of Northern Appalachian Basin is primarily due to flow through fractures and bedding plane separations between strong–weak interfaces of coal measure rocks. Ferguson [22] described a pattern of near-surface fractures and bedding plane separations that he attributed to stress-relief fracturing (Fig. 2). They are generated when neighboring, supporting rocks are removed by erosion. This pattern involves vertical fractures parallel to the valleys and situated in valley floors. Subsidence caused by longwall mining results in tension and compression of the near-surface zone, increasing or decreasing the fracture transmissibility. Wyrick and Borchers [23] reported that groundwater flow associated with stress-relief fractures occur in the valley bottoms and valley sides. Stoner et al. [24] also showed that the permeability of the undisturbed rocks overlying the Pittsburgh coal bed decreases by a factor of ten for each 100 ft (30.3 m) of depth in SW Pennsylvania, specifically in Green County, in SW Pennsylvania. They also found, based on aquifer tests and historical well drilling practice, that the local groundwater system roughly parallels the surface at a depth of 150–175 ft. However, these depths may show local variations according to where the wells are drilled and according to the seasonal precipitation.

In SW Pennsylvania, the hills constitute hydrologic islands. A separate groundwater flow system exists within each hydrologic

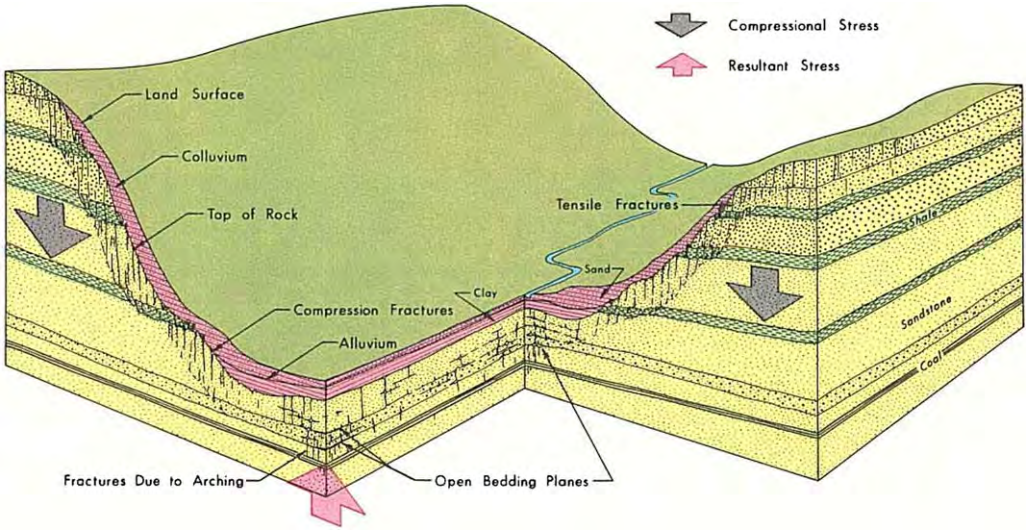

Fig. 2. Block diagram of generalized geologic section showing stress-relief fracturing [23].

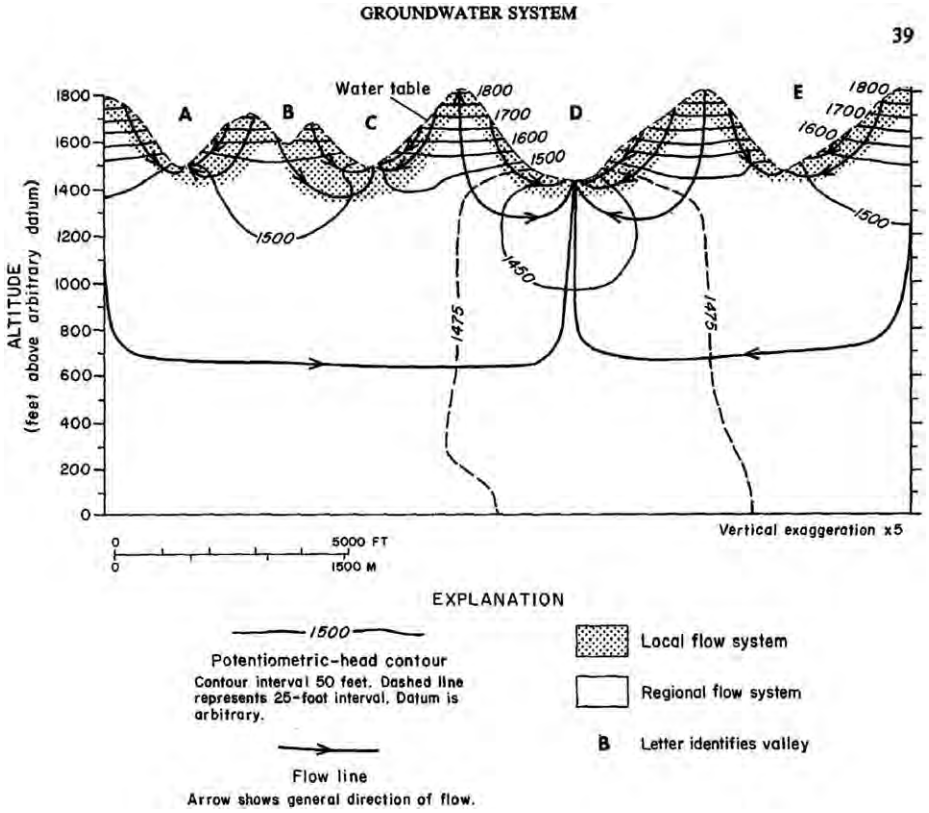

Fig. 3. A model showing the potentiometric head computed from a steady-state model for bituminous coalfields of Greene County, Pennsylvania [24].

island. They are hydrologically segregated from the local groundwater flow system in adjacent islands (Fig. 3). The base of the local flow system is defined by the maximum depth at which groundwater originating within the hydrologic island will flow upward to discharge in the adjacent stream valley. Recharge to the local system is completely from within the hydrologic island. The local system discharges into the adjacent system valleys with some leakage into the deeper intermediate and regional groundwater flow systems. In areas adjacent to larger systems and rivers, local groundwater that leaks downward may commingle with intermediate, even regional flow, which rises to discharge within the valley (Fig. 3). Among all the topographic positions, wells in the valleys have higher change of success of producing high yields due to fracturing beneath the valley bottom. This fracturing is expected to diminish beneath the adjacent hills, thereby limiting the effective areal extent and yield of such aquifers.

3. Downhole monitoring of GGVs

The production performance of GGVs can be closely related to their locations, advances of the longwall face, borehole completions, wellhead designs, and operation of the exhausters. The other important factor that affects the performance of GGVs and the success of methane control is the presence of horizontal and vertical fractures created underground during longwall mining and their hydraulic conductivities for fluid flow.

For the characterization of both the fracturing of underground strata and the resultant changes in hydraulic conductivity in the GGVs during longwall mining, seven boreholes were instrumented with submersible pressure transducers equipped with self-contained data loggers at a mine site in SW Pennsylvania. Two of these were monitoring boreholes drilled as part of NIOSH's monitoring-borehole experimental program performed in 2006–2007. These boreholes will be called MBH-1 and -2 hereafter, throughout this paper. MBH-1 and -2 were 50 ft apart from each other and were drilled to depths of 721 and 755 ft, respectively, in Panel A (1450 ft wide; 11335 ft long) to monitor two different horizons above the Pittsburgh coal bed. The bottom of MBH-1 was 106 ft and the bottom of MBH-2 was 72 ft above the top of the Pittsburgh coal, which was at a depth of 827 ft at that location. This is compared to the 40–45 ft distance above top of coal for the regular GGVs that the mine drilled. The monitoring boreholes were completed with the regular GGV completion standards except the bottoms were cased with 30 ft slotted pipe for MBH-1 and with 20 ft slotted pipe for MBH-2, instead of the conventional 200 ft slotted pipe utilized in GGVs. The experimental boreholes were instrumented to monitor static pressure and gas concentration changes in the borehole, as well as water level changes in the boreholes as they were fractured during mining. Water levels were tracked using downhole transducers and were used to calculate permeability changes in rock formations. A similar approach was used for similar purposes in the gob GGVs drilled in B (1450 ft wide; 11973 ft long), C (1450 ft wide; 4609 ft long) and D panels (1450 ft wide; 11686 ft long). The boreholes instrumented with downhole transducers on these panels were B-3, B-4, C-1, C-2, and D-1.

Fig. 4 shows the locations of the boreholes on a 3-D surface contour map generated from the surface elevation data. In this graph, only the panels where the instrumented boreholes were located are shown. The figure shows that GGVs were drilled at different topographic locations with cold colors representing the higher locations with respect to a datum, which was selected as sea level in this study. As the figure shows, most of the boreholes were drilled on either a hill side or a hill-top with two of them (5B-3 and 6B-2) drilled on valley bottoms. The differences in surface elevations of drill locations change the total drilling depths of the wellbores as the top of the Pittsburgh seam was nearly horizontal at those locations. Table 1 shows the drilling and completion details of the boreholes monitored for this study.

The downhole transducers recorded water head data in the boreholes as the mining face approached and undermined the

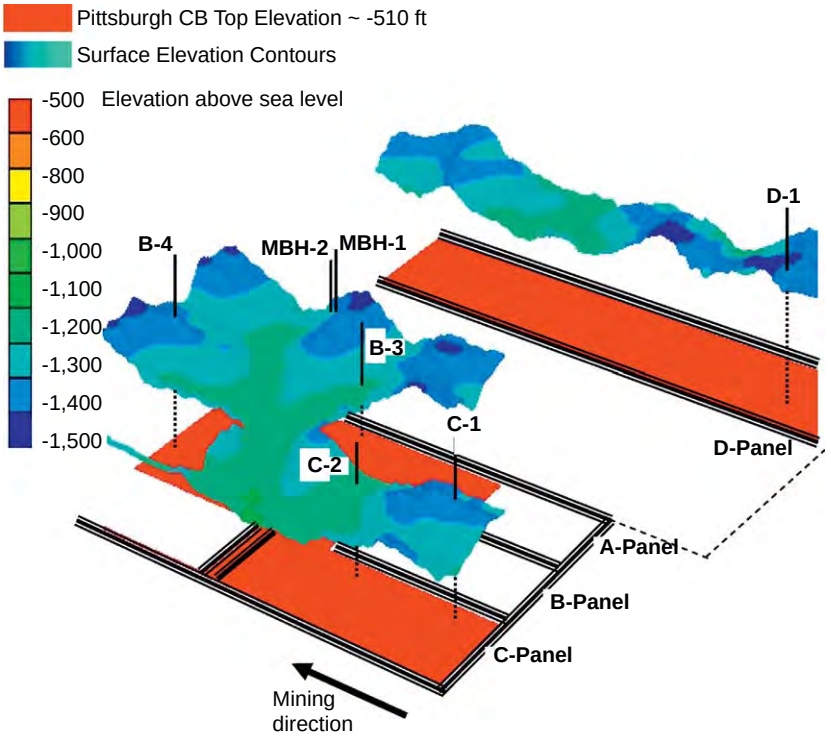

Fig. 4. Location of the boreholes on surface topography over the longwall panels. Sea level is zero. Above-sea-level elevations were taken as the negative direction.

Table 1
Monitored boreholes in mining areas and their completion and instrumentation parameters.

Borehole	Distance from startup (ft)	Distance to TG (ft)	Total depth (ft)	Depth of slotted casing (ft)	Overburden to top of coal (ft)	Bottom of slotted casing to coal (ft)	Transducer depths (ft)	Surface elevation (ft)
MBH-1	4630	330	721	691	827	106	700	1377
MBH-2	4680	330	755	735	827	72	710	1364
B-3	4535	321	588	388	628	40	577	1155
B-4	6535	330	760	560	800	40	562	1325
C-1	460	370	802	602	842	40	736	1350
C-2	2369	330	627	427	667	40	531	1150
D-1	375	330	742	542	782	40	669	1296

borehole location. This data were later used to calculate the changes in hydraulic conductivity and transmissibility of overlying formations within the slotted sections of the boreholes. This data, together with face location, face advance rate, stratigraphy, and the completion parameters of the boreholes can be used to predict how the fluid flow-related properties of the formation may change and how the borehole location can be adjusted to drill the boreholes in the most permeable location for increased capture of released methane. Downhole instrumentation in the boreholes also helps to see if there is any water build-up in the boreholes after undermining; as this may adversely affect the operation of the exhauster pump. The setting depths of the transducers in the boreholes are given in Table 1.

4. Longwall face advance rates during the tests

The fractures and permeability enhancements in GGVs during longwall mining may be closely related to dynamic deformation, progression of subsidence, and settlement of the fragmented roof mass. The main factors influencing the dynamic deformation process are average mining height, overburden depth, face length, rate of face advance, and residual effects from old mining activities and face stoppages. Some of these have been discussed in the previous sections. In addition to these, regulating the face advance rate in longwall mining was proposed as an effective means of reducing the disturbance potential to surface structures associated with subsidence process [9]. However, there are seemingly two opposite views about the effects of the face advance rate on the magnitudes of dynamic deformations. In the US, the common belief is that a faster and constant face advance rate produces smaller dynamic deformations, whereas in Germany, it is thought that a slow rate is more beneficial to surface structures [9]. Thus, advance rate may be effective also on the underground deformation and on the enhancement of hydraulic conductivity around gob gas boreholes.

In order to be able to evaluate face advance history as a parameter in evaluation of hydraulic conductivities of the boreholes and to gain some insights on flow potential of the boreholes, the face advance rates reported by the mining company during longwall operation of A–C panels as well as D panel were analyzed. In these analyses, daily advance rates and the periods when the boreholes were intercepted were evaluated. Also, in order to match the downhole transducer data with the face location and borehole location, the dates before and after borehole interception were plotted as a function of face location from panel start and polynomials were fit to those data. These equations were used to match the location of the face at a given time and day with the corresponding downhole pressure data recorded by the transducer. Fig. 5 shows, as an example, the history of face advance rate during mining of B panel, borehole interception intervals and how the analyses described above were performed.

Fig. 5a shows the history of face advance rate during mining of B panel. The total mining days, including two weeks of miner's vacation, was around 325 days for this panel. The daily advance rates during mining were around 40 ft/day (Fig. 5a), except a slower period with rates of 20 ft/day around the 250th day of mining. However, a majority of advance rates were in the 35–65 ft/day range, where faster advances were achieved at the beginning and end of the mining. B-3 and -4 were intercepted between 90–95 days and 148–157 days from start of mining, respectively (shaded areas in Fig. 5a). During these time intervals, mining rates were generally around 30 ft/day and 50 ft/day for B-3 and -4, respectively (Figs. 5b, c).

Quadratic equations were fitted to face location versus mining days. Equations shown in Figs. 5b and c and also given in Table 2 indicate that the data can be represented by these equations with a regression coefficient (R^2) of more than 0.99. These equations can also be used to find the rate of face advance at a given day by taking the derivative of the equations. The equations obtained using the similar approach for all other monitored boreholes are collectively given in Table 2.

5. Estimating the location of bedding-plane fractures occurring during mining

Horizontal fractures occur along weak–strong rock layer interfaces in the movement of the overburden. The formation, thickness and location of horizontal fractures influence the hydraulic conductivity of the overburden strata, which creates methane emission pathways and controls methane emissions into the mine. Thus, the ability to estimate the location and magnitudes of the fractures and their hydraulic flow properties are important for placement of boreholes and, consequently, for controlling methane more effectively.

Palchik [5] has shown that the extent of fractured zone induced by mining in the Donetsk coal basin can be determined based on the change in natural methane emission from this zone. After a modification to the earlier tests system, he [25] was able to locate the individual fractures at bedding plane separations. The method was based on isolation of each methane emission zone in a borehole by measuring the pressure and flow rate and correlating these zones with the strata logs. Further, the presence and absence of estimated horizontal fractures was correlated with uniaxial compressive strength and thickness of rock layers, distances from the extracted coal seam to the rock layer interfaces, and the thicknesses of extracted coal seams. Observations on the presence and absence of horizontal fractures at different rock layer interfaces of the overburden showed that the probability increased with increasing compressive strength difference of neighboring rock layers as well as decreasing distance of the layer from the mined coal bed.

In this paper, a similar approach was adapted for the rock layers in the overburden of the Pittsburgh coal at the studied mine

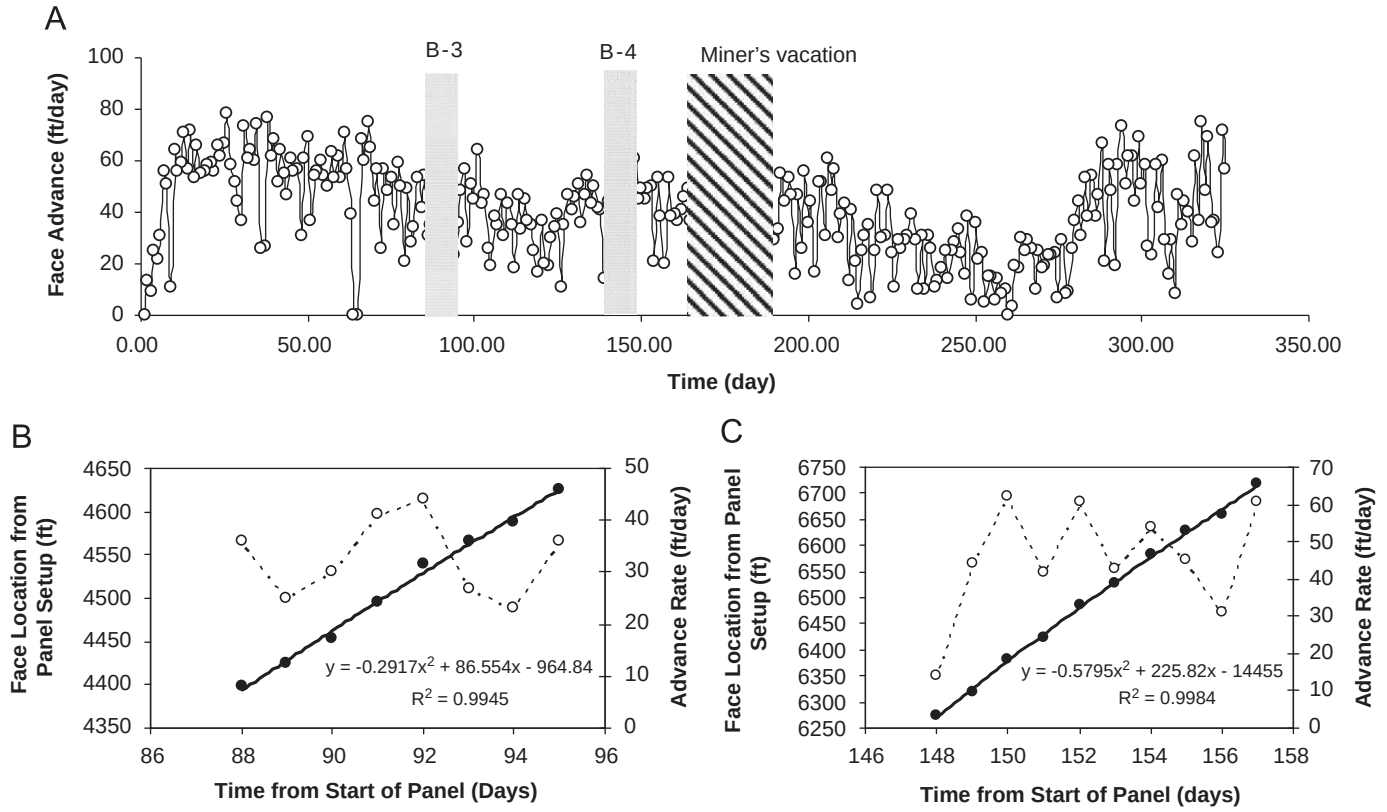

Fig. 5. Daily face advance rates (a) and face location relations (b, c) for B-3 and -4 as the face approached to their locations. In these figures, dashed lines are the daily advance rates, where continuous lines are the face distances from panel setup.

Table 2
Face location versus time relations developed for monitored boreholes in panels A–D.

Boreholes	Face position vs. mining days–[Eq. (θ)]		1st derivative of Eq. (θ)
MBH-1	$y = -0.8541x^2+196.98x-6302.8$	$R^2 = 0.99$	$dy/dx = -1.7082x+196.98$
MBH-2	$y = -0.8541x^2+196.98x-6302.8$	$R^2 = 0.99$	$dy/dx = -1.7082x+196.98$
B-3	$y = -0.2917x^2+86.554x-964.8$	$R^2 = 0.99$	$dy/dx = -0.5834x+86.55$
B-4	$y = -0.5795x^2+225.82x-1445$	$R^2 = 0.99$	$dy/dx = -1.1590x+225.82$
C-1	$y = -1.4702x^2+76.78x-401.48$	$R^2 = 0.98$	$dy/dx = -2.9404x+76.78$
C-2	$y = -0.2995x^2+79.99x-1305.8$	$R^2 = 0.99$	$dy/dx = -0.5990x+79.99$
D-1	$y = -1.5714x^2+90.31x-902.2$	$R^2 = 0.99$	$dy/dx = -3.1420x+90.31$

The derivatives of the equations (advance rate) are also presented.

site by imposing the lithology and thickness information obtained from nearby core logs to GGV locations after a depth correction. The depth correction procedure allowed the rock layers, the slotted casing locations, the transducer positions, and all other depth and borehole completion information given in Table 1 to be compared in the same depth scale as shown in Fig. 6.

Fig. 7 shows a plot of the ratio of thickness of each layer to extracted coal bed thickness and their heights relative to the top of the extracted coal bed. This graph also shows the strata identifications as sandstone, limestone, and weak strata (coal, shales of all kind and clay stones). Palchik [25] has noted, based on the field measurements, that separations at the interfaces and formation of fractures may be restrained by thick and strong rock layers, called "bridge layer", in the overburden. The "bridge layer" in the study area is the thick limestone close to the top of the overburden section shown in Fig. 6. According to Palchik [25], the probability of bedding plane separation along the rock layer interfaces decreases with increasing height above the coal seam (H) and with increasing thickness of the bridge layer. According to this concept and these observations, the probability of fracture development and bedding plane separations along the bridge layer (if it exists) at the study site is less, as marked on the upper right section in Fig. 7. Furthermore, it was observed that the probability of forming a fracture or bedding plane separation increases as the height above the coal bed (H) and the ratio formation thickness (h) to the coal seam thickness (m) decrease. Therefore, in the study boreholes, it is more probable that such deformations will occur within an interval between 40 and 145 ft from the top of coal bed and up to h/m of 4 (Fig. 7). This interval contains thinner limestones, sandstones, and weaker strata, such as coal beds and shales (Fig. 6).

Fig. 8 shows the ratio of the thickness of top layer (h_t) to the bottom one (h_b) for each interface, calculated in pairs, along the stratigraphic sections shown in Fig. 6, versus the height of the interface from the top of the Pittsburgh coal bed (H). In this figure, the types of the interfaces were also defined with different-colored markers. Palchik [25] has reported that when the strata thickness ratio (h_t/h_b) is low (<2), there are very few horizontal

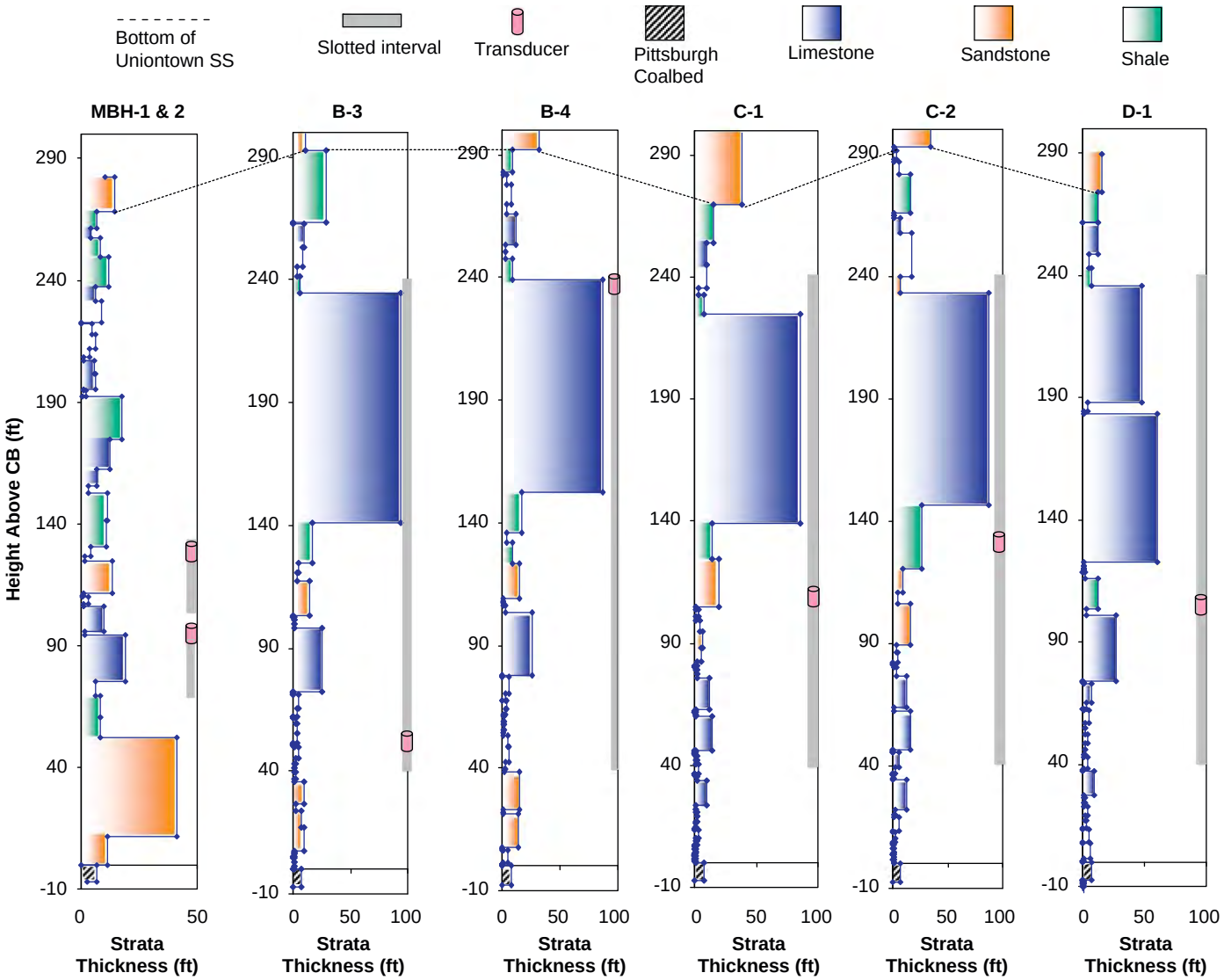

Fig. 6. Stratigraphic log and thicknesses of the formations at each borehole locations after correction to sea level.

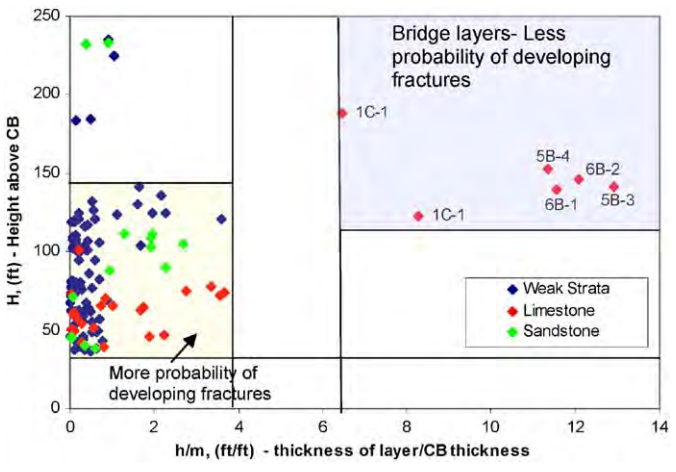

Fig. 7. Height of the layers above coal bed versus the ratio of their thicknesses determined from data of Fig. 6. This graph shows the distribution of different rock types and the regions where fracturing probability is higher within strata.

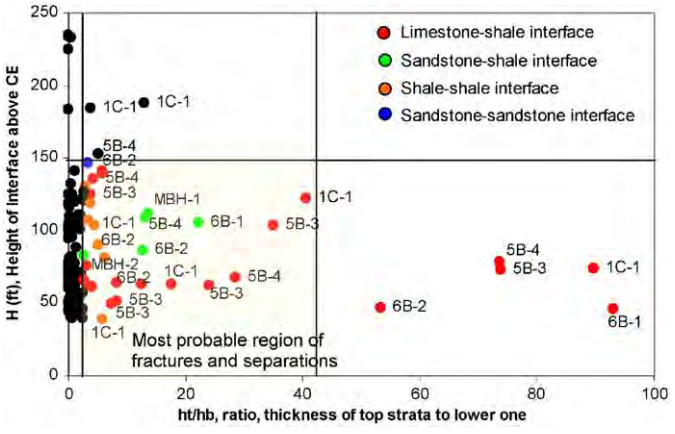

Fig. 8. Height of the formation interfaces from coal bed versus the thickness ratio of sequential layers in the strata column (Fig. 6). This graph shows the types of the interfaces and the region where fracturing and bedding plane separation will likely to occur. Black dots are where separations are not expected due to height ratios and interface characteristics.

fractures. In order to apply a similar concept for the strata in our tests sites and to determine the lower limit of strata-thickness ratio for fracturing or bedding plane separations to occur, we have used water drop data measured in MBH-1 and -2. In all the water tests conducted, the minimum numbers of interfaces were in MBH-1 and -2, since they have the shortest slotted casings (30 and 20 ft, respectively) at heights of 72 and 106 ft above the coal seam. However, we still measured water drop in these boreholes as mining approached. This suggests the development of horizontal fractures in these intervals. Therefore, the strata thickness ratios in these interfaces in MBH-1 and -2 were used as the lower boundary for horizontal fractures to occur. It was observed that this boundary matches well with what Palchik [25] reported. As for the upper boundaries for strata thickness ratios, the previous discussion on bridge layers and the heights above coal bed were used. Thus, it was estimated that the horizontal fractures in the study area were likely to occur in limestone–shale, sandstone–shale and shale–shale interfaces between $40 < H < 150$, and $2.5 < h_t/h_b < 42$. Fig. 8 also shows the fracture region in each borehole and the type of interface.

6. Hydraulic conductivities

6.1. Observed flow responses in the boreholes

The water–head drop and resultant pressure decline with small data collection intervals created a highly resolved data file in terms of time and water level. Analyzing the file as it was uploaded from the transducer resulted in too many values of the same flow period leading to a noisy result. Thus, in order to eliminate these adverse effects, the data points (time and water head pressure) at the beginning and at the end of each flow period were determined by the change of slope of data trend. Fig. 9 shows these data as time versus normalized (with respect to initial water head) water head for each of the boreholes.

Figs. 9a–d show that the change in the water level in the borehole with time formed a variable flow trend until water completely drained from the borehole during mining. These variations indicate the changes in hydraulic conductivity and the variation in the heterogeneity in the strata.

Various factors may control the hydraulic properties of a porous medium and the calculated hydraulic conductivities. The factors such as mechanical skin, layering and anisotropy were investigated analytically and numerically [26,27]. In addition to skin effects, formation heterogeneity may influence test results. Moreno and Tsang [28] showed numerically that preferential flow paths tend to develop in extremely heterogeneous media. Mean hydraulic properties along such channels or fractures may be significantly higher than the rest of the porous medium. In a more recent paper, Maher and Donovan [20] investigated the relationship between extreme heterogeneity and hydraulic test results in a mine-spoil aquifer created by backfilling the excavations during surface mining. They have observed three different drawdown response types during the tests: conventional, rapid response and "double" response. The "double" response curve was characterized by an initial rapid drawdown for the first 10% of the data, followed by a slow period similar to a conventional behavior. The differences in responses were interpreted as the boundary effects, as either steepening or flattening of the response curve. Steepening was reported as a result of hydraulic boundary or heterogeneity effects near the borehole, whereas flattening was interpreted as either leakage, recharge, or slow vertical drainage from unconfined storage. They also conducted numerical experiments to examine the effects of different heterogeneities on the response curve. They observed that increasing the skin porosity, skin storage and skin conductivity produced "double-flow" type response.

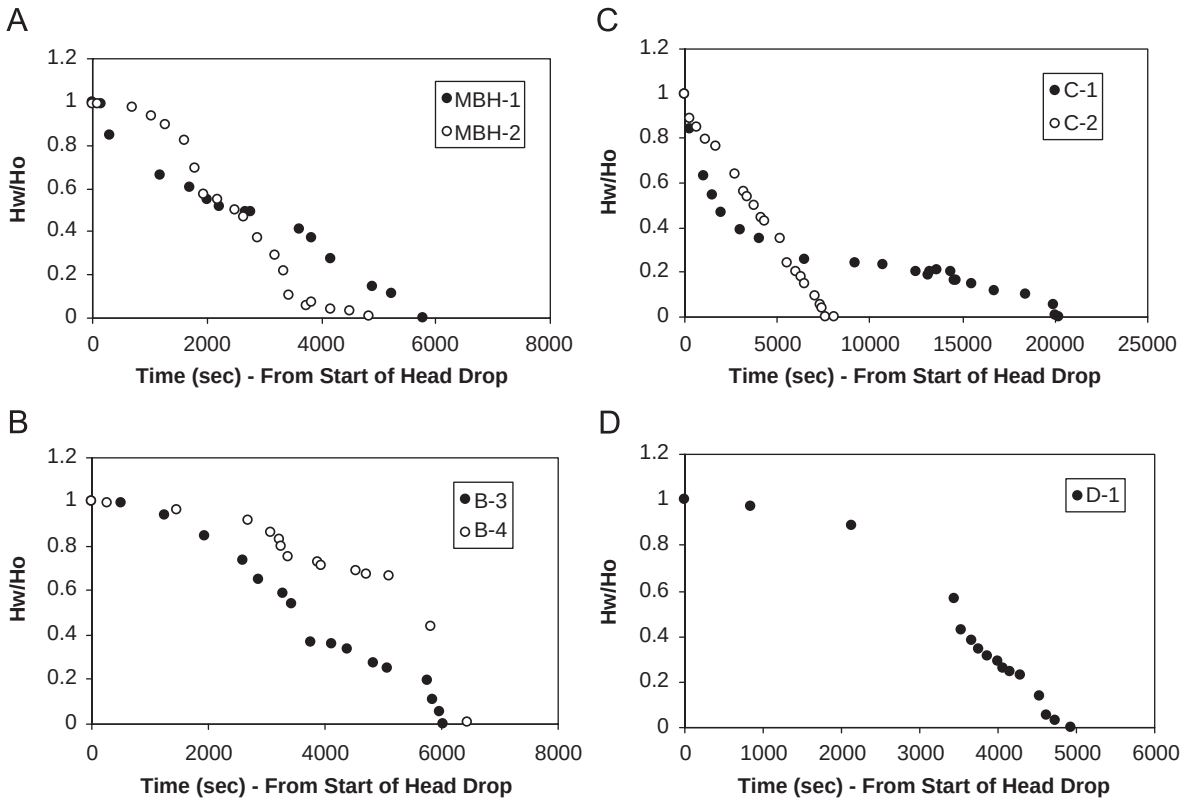

Fig. 9. The change in the water level (normalized head) in the boreholes with time.

Fig. 9 show the observed flow responses measured in our tests and indicate the existence of "multiple" flow periods in the wells. Although the tests and the response curves are much more complicated than the cases explained before, the observed flow responses are characteristic of heterogeneous formations. These double-flow data plots may be representative of initial saturation of opening (dilating) fractures, followed by a slowed decline as the water drains in the now saturated fracture also. The measured variations in drawdown were most likely caused by changing hydraulic conductivities resulting from a combination of factors such as position of the face relative to the borehole, topographic location of the borehole and completion parameters, strata characteristics and variation in mining advance rate.

6.2. Hydraulic properties of the overburden during mining

6.2.1. Hydraulic conductivity and transmissibility

Hydraulic conductivity is the proportionality constant in Darcy's law, which relates the amount of water which will flow through a unit cross-sectional area of aquifer under a unit gradient of hydraulic head. The hydraulic conductivity (K) is specific to the flow of a certain fluid. This means that, for example, K will go up if the water in a porous medium is heated (reducing the viscosity of the water), but κ will remain constant. The two are related as follows:

$$K = \frac{\kappa\gamma}{\mu} \tag{1}$$

where K is the hydraulic conductivity [LT^{-1}], κ is the intrinsic permeability of the material [L^2], γ is the specific weight of water [$ML^{-2}T^{-2}$], and μ is the dynamic viscosity of water [$ML^{-1}T^{-1}$].

The transmissibility, T, of an aquifer, on the other hand, is a measure of how much water can be transmitted horizontally such as to a pumping well

$$T = Kb \tag{2}$$

Transmissibility is directly proportional to the aquifer thickness (b).

6.2.2. Methods of calculating hydraulic properties of the overburden during mining

In order to calculate the hydraulic conductivities based on the water drawdown data presented in Figs. 9a–d, two models were used. These models were those of Cooper, Bredehoeft, Papadopulos [29] and Bauwer and Rice [30]. Cooper et al. [29] calculated aquifer values by overlying the field data to a family of curves as shown in Fig. 10. The field data was moved towards the type curves in such a way that the axes were parallel to each other until the best type curve was found which matched the field data. As in all type curve matching procedures, the decision of the best match is usually subjective and only a noise free, perfectly homogeneous response data can be closely matched to theoretical curves. In most cases, either the early or the later portion of the field data has to be ignored to be able to match the rest of the data points to one of the curves, making this rather undesirable. In extreme cases of heterogeneity, as in the data measured for this study, the matching procedure is more difficult and more prone to error. Due to concerns of the nature of the field data and the sources of errors explained in the previous paragraphs, this technique is not used further in this analysis. Note that in Fig. 10, the field data are shown at a stage before moving them towards the type curves in order not to make this figure too crowded. In Fig. 10, H_w/H_o is the dimensionless drawdown in the borehole, $\alpha = Sr_w^2/r_c^2$ is the dimensionless storativity, and $\beta = Tt/r_c^2$ is the dimensionless time, where S is the storativity, $T = Kb$ is the transmissivity, and r_c and r_w are the casing and well radii, respectively.

Alternatively, the Bauwer and Rice [30] method was used on the field data to calculate the hydraulic conductivities between consecutive data points, for the intervals of the response curve that follow a similar flow behavior (points falling on the same straight line), and for the average of all data points. This model applies to the injection or withdrawal of a volume of water from the well casing, where hydraulic conductivity (K) is defined as

$$K = \frac{r_c^2 \ln(R/r_w) \ln(H_o/H_w)}{2(l-d)t} \tag{3}$$

Bauwer and Rice [30] determines the radius of influence, R, for different values of r_w, in terms of (l–d), r_w, H_w and m (aquifer

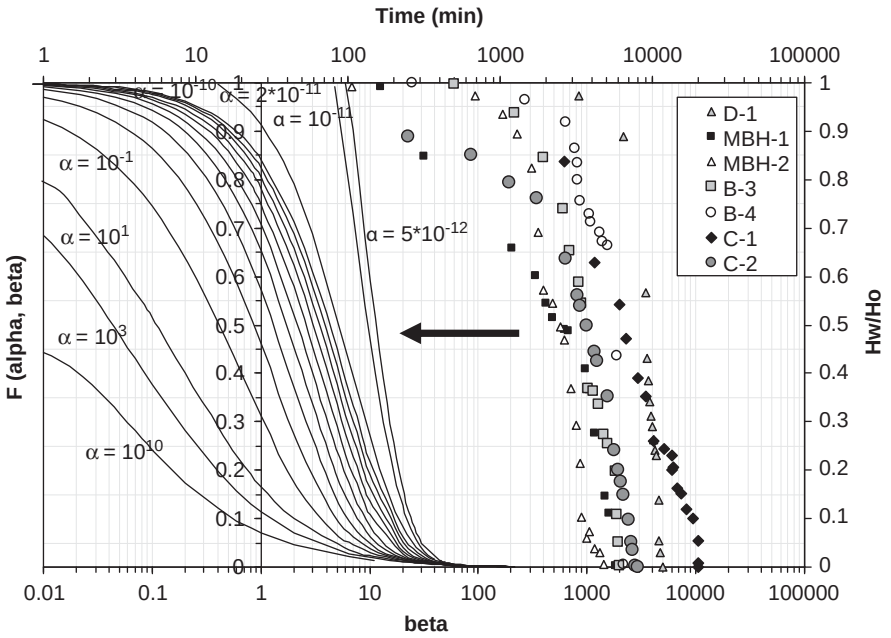

Fig. 10. Plot of the type curves generated using Cooper et al. [29] model and the experimental data obtained from boreholes. Arrow shows the direction to which experimental data should be moved for type-curve matching.

Table 3
Average hydraulic conductivity (K) and transmissibility (T) values determined for different aquifer depths from surface using Bauwer and Rice [30] method.

MBH-1		MBH-2		B-3		B-4		C-1		C-2		D-1	
50		50		50		50		50		50		50	
K	2.52E−03	K	3.26E−03	K	4.40E−04	K	1.54E−04	K	5.22E−04	K	7.18E−04	K	7.05E−04
T	1.957	T	2.529	T	0.249	T	0.115	T	0.412	T	0.443	T	0.515
200		200		200		200		200		200		200	
K	2.47E−03	K	3.20E−03	K	4.23E−04	K	1.50E−04	K	5.12E−04	K	6.95E−04	K	6.86E−04
T	1.547	T	2.005	T	0.176	T	0.089	T	0.328	T	0.323	T	0.399
400		400		400		400		400		400		400	
K	2.37E−03	K	3.09E−03	K	4.36E−04	K	1.42E−04	K	4.89E−04	K	6.43E−04	K	6.49E−04
T	1.010	T	1.318	T	0.094	T	0.056	T	0.215	T	0.171	T	0.248

[K in ft/day; T in ft2/day]

saturated thickness) using with an electric resistance analog model. From the experiments, the following empirical equation was developed for estimating R:

$$\ln(r_w/R) = \frac{1.1}{\ln(r/r_w)} + \frac{A + B\ln[(m-l)/r_w]}{(l-d)/r_w} \quad (4)$$

where A and B are dimensionless coefficients that are function of $(l-d)/r_w$ for the partial penetration case. If the well fully penetrates the aquifer, in that case the appropriate equation for $\ln(r_w/R)$ is

$$\ln(r_w/R) = \frac{1.1}{\ln(l/r_w)} + \frac{C}{(l-d)/r_w} \quad (5)$$

A more complete explanation of these coefficient and solutions for some specific cases can be found in Dawson and Istok [31]. However, one important aspect of this method should be mentioned: the calculated K is dependent on the thickness open to flow, (l–d). This is important in comparative studies where the length of open-to-flow section of the boreholes varies. Also, this method has more representative assumptions in its application to the current study, including the leaky and unconfined aquifer. Thus, the method of Bauwer and Rice [30] was used for the rest of the calculations and for the interpretations of the results in this paper.

6.3. Selection of aquifer depth for calculations

The Bauwer and Rice method [30] was used to calculate the average hydraulic conductivities and the transmissibilities for each borehole at different depths of the initial water table. The variations in water table depths may depend on seasonal variations in precipitation as well as the location of the borehole. As it was presented in the groundwater hydrology section, the water table, although it usually may be parallel to the ground surface, can be at a shallower depth at the valley bottoms. Thus, the boreholes drilled at valley bottoms may hit the water aquifer at shallower depths than the hill-top wells. Also, the hydraulic properties of the formations at valley bottoms may be different due to stress-relief fracturing (Fig. 2).

This method was used to quantify hydraulic conductivities and transmissibilities for different aquifer thicknesses at each borehole location. Calculations were conducted for cases where the water table was 50, 200, and 400 ft below the surface. Because the bottom of the Pittsburgh coal is considered the base of the aquifer for local-regional flow system, increasing water table depth decreases aquifer thicknesses (Table 3). As this table shows, hydraulic conductivities are not affected by the thickness of the aquifer, whereas transmissibilities decrease as the thickness of the aquifer decreases (400 ft case). In these analyses, 200 ft was selected as the depth of a static water table for all boreholes, this value being in close agreement with the values of 150–175 ft reported by Stoner [24] for depths in SW Pennsylvania. Thus, the calculations and the discussions on the changes in hydraulic properties of the overburden during mining in the next sections will be based on the K and T data calculated using the Bauwer and Rice [30] method and 200 ft as the depth of the aquifer. It should be mentioned that the K-value estimated from slug testing is dependent in some cases on the thickness of the part of the aquifer in which flow occurs due to a slug input or another external changes [17]. Since the slotted casing is the only open-to-flow section of the boreholes in the overburden, their lengths would make a difference. In fact, the shorter the slotted section, the higher the K-value as observed in MBH-1 and -2 in Table 3. Thus, the calculated values will be normalized to a conventional 200 ft slotted casing used in the GGVs.

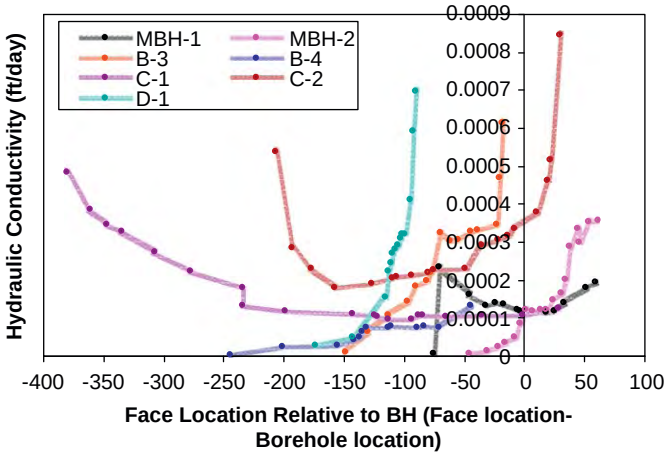

Fig. 11. Change of hydraulic conductivities calculated from borehole tests as a function of longwall face location relative to borehole location.

6.4. Change of hydraulic properties of overburden during mining

This section describes the hydraulic conductivities calculated from downhole instrumentation data. Fig. 11 shows the variation in hydraulic conductivities as a function of face location with respect to borehole location. In this graph, negative values

represent a face location before it reaches the borehole location, where as positive values represent the location of the face after undermining. A value of zero represents the longwall face under the borehole location. This figure suggests that hydraulic conductivities change based upon the borehole monitored. At C-1 and -2, initial hydraulic conductivities were high when the effects of the approaching face were first felt in each borehole and started to decrease as the face approached the boreholes. The values started increasing as the face approached and eventually undermined the borehole (Fig. 11). One noticeable difference is that the hydraulic conductivity values show that the strata around C-1 started fracturing when the face was approximately 375 ft away. In B-3 and -4 boreholes (also in D-1 too), initial hydraulic conductivities were low but followed an increasing trend as the face approached the borehole locations. These behaviors suggest that differences exist in overburden fracturing mechanisms.

When we compare the geology of C-1 with -2, and also the locations of the transducers in these two wells, we see that they are very similar (Fig. 6). However, C-1 was the first borehole in the panel, was close to the setup entry, was located at a higher elevation, and thus had a thicker overburden (Table 1) compared to C-2. This may suggest that the first borehole in the panel is fractured earlier than the other boreholes drilled close to the middle or end of the panel. Also, the weight of the overburden (hilltop versus valley bottom wells) and the differences in existing stresses and how they interact with mining-induced stresses under these topographical features may create differences in the way that the boreholes fracture during undermining. Regardless, the general observation, without taking the topography into account, is that from setup entry to the first weighting as the face moves, the roof experiences elastic, plastic deformation, failure and development of vertical fractures [6]. Since the first weighting does not occur immediately and usually not until one face width of advance, the roof strata continues to cantilever, opening existing fractures and creating new bedding plane separations ahead of the face. After the first weighting as the overburden caves, fractures develop ahead of the face. Separated vertical fractures occur at higher levels and horizontal and vertical fractures occur at the lower ends of fractured zone. After the face advances to a certain distance, fractures and broken rocks are compressed.

B-3 and -4 were located close to the middle of the panel and gob. A comparison of their stratigraphic logs with the ones in panel D shows that there was a 30 ft-thick sandstone layer on the top of the immediate roof of the Pittsburgh coal bed in C panel (Fig. 6). According to Palchik [5], the ratio between the maximum height of the zone of interconnected fractures and the thickness of the extracted coal seam increases with the increasing number of rock layers and decreases with the stiffness of the immediate roof. This may explain the differences in the changes of hydraulic conductivities in boreholes between panels B and C. In panel C borehole locations, the immediate roof of the Pittsburgh coal bed was mainly thin shale layers and rider coals up to 20 ft from the coal bed (Fig. 6). These thin and weak layers must have broken very easily and initiated fracturing of the limestone intervals above, thus increasing the height of the fractured zone and increasing the hydraulic conductivity. On the other hand, in panel B, the stiffer sandstone layers probably did not break easily, limiting the increase in their hydraulic conductivities. As the sandstone failed in a transient mode, hydraulic conductivities increased slowly from low values to higher ones.

Furthermore, B-3 was located in a valley, whereas B-4 was located at a hilltop (Fig. 4). Thus, B-3 had a higher hydraulic conductivity as it was observed in C-2, probably due to it location. On the other hand, B-4 started fracturing earlier but had a lower hydraulic conductivity when the water in the borehole drained completely. This may suggest that the location of borehole and the overburden weight on the fractured strata did not promote high conductivities.

The completion parameters of MBH-1 and -2 in panel A were different from regular GGVs; as they had shorter slotted casings. The distances to the Pittsburgh coal bed from the bottom of the slotted casings were 106 and 72 ft for MBH-1 and -2, respectively (Table 2). They had a thick sandstone layer as the immediate roof. It is probably due to this stiff roof material that the fracturing of the strata was delayed until the face was within 50–100 ft of the borehole. The slotted casing in MBH-1 was located against a weaker section with more strata interfaces compared to MBH-2 which was located against a more competent layer with fewer interfaces (Fig. 6). Although MBH-1 was higher in the strata, it was fractured more effectively at the beginning, compared to MBH-2, which was fractured later and with hydraulic conductivities increasing slowly.

6.5. *Effects of overburden, face advance rate and distance from the panel setup on hydraulic conductivities*

In order to investigate the effects of overburden thickness, face advance rate and the distance of the GGV from the panel setup entry, the average values of the hydraulic conductivities presented in the previous section were calculated. The comparisons were based on these average values.

Fig. 12 shows the variations in average hydraulic conductivity for different boreholes and their respective overburden thicknesses. As the figure shows, there are mainly two regions of overburden thickness in which the conductivities were clustered. The first region contains boreholes with higher average hydraulic conductivities with overburden thickness up to around 775 ft. The boreholes in this interval are B-3, C-2, and D-1. These boreholes are the ones drilled in valley bottoms (B-3 and C-2), thus with less overburden, and the first borehole in D panel (D-1). Comparing hydraulic conductivities with only one independent variable (overburden) suggests that the boreholes in valley bottoms are going to be more productive in producing methane. Also, the first borehole in a panel can be as productive unless the overburden at its location is too thick, as it was in the case of C-1.

Fig. 13 compares the average hydraulic conductivities developed in the boreholes with the average face advance rates during mining of their locations. The distribution of the values as a function of face advance rate suggests that as the rate of advance increases, the hydraulic conductivities developed in the boreholes tend to decrease. Keeping all other variables constant, this can be

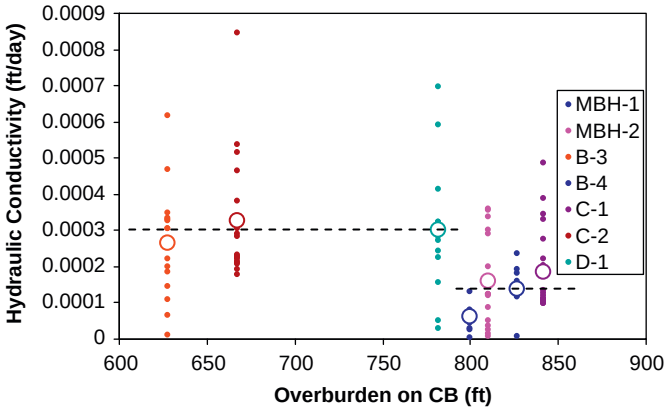

Fig. 12. Average hydraulic conductivities in each borehole as a function of overburden thickness at the borehole locations. Hollow markers are the averages for each borehole.

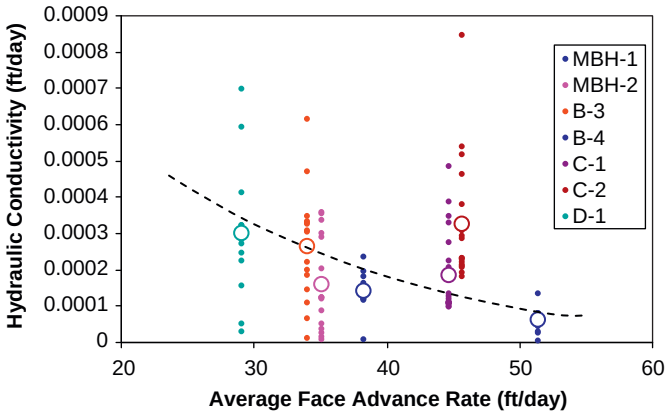

Fig. 13. Average hydraulic conductivities in each borehole as a function of average face advance rates during mining of the borehole locations. Hollow markers are the averages for each borehole.

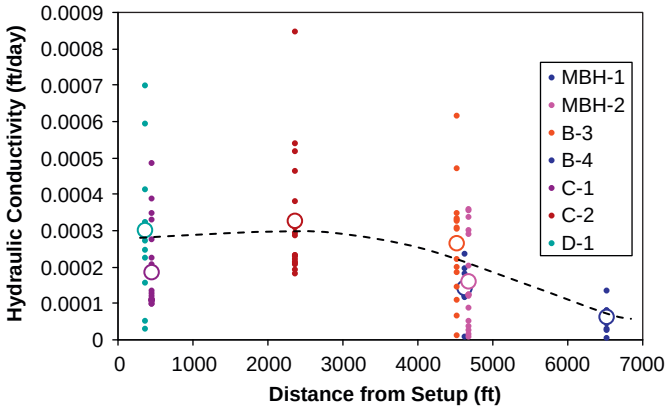

Fig. 14. Average hydraulic conductivities in each borehole as a function of distances of the boreholes from panel setup entry. Hollow markers are the averages for each borehole.

explained by the fact that at a higher face advance rate, subsidence occurs at a higher rate. This increases the maximum slope, horizontal displacements, and the change of dynamic stress from tensile to compressive, which in a fractured rock mass accelerates the settlement [9]. Higher settlement rates and compressive stresses decrease hydraulic conductivity in the borehole. On the other hand, a slower advance rate could induce a high dynamic tensile stress in front of the face before converting to compressive stress some distance behind the face. The prolonged tensile stress at high levels possibly creates more fractures and bedding plane separations. This could increase the hydraulic conductivity of the formations within the borehole interval.

Fig. 14 illustrates the effects of distance of the borehole from panel setup on hydraulic conductivity values. This figure shows that as the borehole distance from the panel setup entry increases, the hydraulic conductivity is in a decreasing trend. This is possibly due to closure of factures from compaction of gob with successive weightings. This may explain why boreholes drilled at increasing distances from panel setup are traditionally not very productive.

The graphs given in the above discussions show the variation of hydraulic conductivities as a function of only one variable. Although in some cases this type of representation may be informative and helpful, in cases where the dependent variable is affected by more than one independent variable, care should be taken and the modeling should be based on either multivariable regression or artificial neural network type approaches.

7. Summary and concluding remarks

This report presented an integrated study evaluating underground strata and their potential responses to longwall mining. This included evaluations of mining rate effects and data obtained from in-situ slug tests performed in gob gas ventholes to characterize the changes in hydraulic conductivities. Hydraulic conductivities developing in a borehole can help to predict whether the GGV's can produce methane more effectively.

The results indicate that the hydraulic conductivity developments in the boreholes and their potential production performances are affected by the underground strata and the roof materials. In situations where the roof material is stiff and thick, it cantilevers behind the shields leading to a lesser degree of fracturing in overlying strata. This may decrease development of high permeability fractures around the borehole.

In this study a double-flow behavior, in water drop during slug tests, expected from heterogeneous formations was also observed. The different flow-rate phases and different hydraulic conductivities can be related to initial opening and filling of fractures with fluid and followed by changes in fractures now saturated with fluid. Based on the slug tests and other data used in this study, it was concluded that the locations of the boreholes are important for their fracturing time and for the resultant hydraulic conductivities. Results showed that hill-top boreholes fracture earlier than valley-bottom wells. However, the permeability of the factures in hill-top wells is less compared to valley-bottom wells. These wells may potentially be less productive. It was shown also that greater overburden depths cause lower hydraulic conductivities and potentially less effective boreholes as opposed to shallow GGVs. It was also observed that the proximity of the boreholes to the start-up entries makes a difference in fracture development too. First boreholes in the panels generally have higher hydraulic conductivities, as opposed to GGVs drilled close to the end of the panel. As the drilling distance to the panel setup entry decreases, average hydraulic conductivities are potentially higher. This may be one of the reasons why the first boreholes are generally more productive. In addition to borehole location, mining advance rate was found to be effective also on the hydraulic conductivities measured using slug tests. It was shown that higher face advance rates at the study mine site result in generally lower hydraulic conductivity in the fractures. This may be due to the rapid change of tensile stresses to compressive ones reducing the fracture conductivity.

The bedding plane separation probabilities can be predicted using the distances of bedding planes to the extracted coal seam and the thicknesses of neighboring layers, as well as the thickness of bridge layer. The prediction techniques based on these information were applied for the coal measure rocks in this study area. It was observed that mostly strong–weak rock interfaces are prone to separation and the probability decreases as the distance from coal seam increases. Also, the thickness of what is called a "bridge-layer" in this paper plays a role in fracture development.

References

[1] Mucho TP, Diamond WP, Garcia F, Byars JD, Cario SL. Implications of recent NIOSH tracer gas studies on bleeder and gob gas ventilation design. In: Proceedings of society of mining engineers annual meeting, Salt Lake City, 2000.

[2] Singh MM, Kendorski FS. Strata disturbance prediction for mining beneath surface waters and waste impoundments. In: Proceedings of 1st international conference on ground control in mining, Morgantown, WV, 1981.

[3] Kendorski FS. Effect of high-extraction coal mining on surface and ground waters. In: Proceedings of 12th international conference on ground control in mining, Morgantown, WV, 1993.
[4] Hasenfus GJ, Johnson KL, Su DWH. A hydrogeomechanical study of overburden aquifer response to longwall mining. In: Proceedings of 7th international conference on ground control in mining, Morgantown, WV, 1988.
[5] Palchik V. Formation of fractured zones in overburden due to longwall mining. Environ Geol 2003;44:28–38.
[6] Li S, Lin H, Cheng X, Wang X. Studies on distribution pattern of and methane migration mechanism in the mining-induced fracture zones in overburden strata. In: Proceedings of 24th international conference on ground control in mining, Morgantown, WV, 2005.
[7] Cui X, Wang J, Liu Y. Prediction of progressive surface subsidence above longwall coal mining using a time function. Int J Rock Mech Min Sci 2001;38: 1057–63.
[8] Luo Y. An integrated computer model for predicting surface subsidence due to underground coal mining (CISPM). PhD dissertation, Department of Mining Engineering, West Virginia University, Morgantown, WV; 1989.
[9] Preusse A. Effect of face advance rates on the characteristics of subsidence processes associated with US and Germany longwall mining. In: Proceedings of 20th international conference on ground control in mining, Morgantown, WV, 2001.
[10] Matetic RJ, Liu J, Elsworth D. Modeling the effects of longwall mining on the ground water system. Report Invest 9561, US Bureau of Mines, Pittsburgh; 1995.
[11] Fawcett RJ, Hibberd S, Singh RN. An appraisal of mathematical models to predict water inflows into underground coal workings. Mine Water Environ 1984;3:33–54.
[12] Liu J, Elsworth D. Three-dimensional effects of hydraulic conductivity enhancement and desaturation around mine panels. Int J Rock Mech Min Sci 1997;34:1139–52.
[13] Gale W. Application of computer modeling in the understanding of caving and induced hydraulic conductivity about longwall panels. In: Proceedings on coal 2005, 6th Australasian Coal Operator's conference, Brisbane, 2005.
[14] Whittles DN, Lowndes IS, Kingman SW, Yates C, Jobling S. Influence of geotechnical factors on gas flow experienced in a UK longwall coal mine panel. Int J Rock Mech Min Sci 2006;43:369–87.
[15] Whittles DN, Lowndes IS, Kingman SW, Yates C, Jobling S. The stability of methane capture boreholes around a longwall coal panel. Int J Coal Geol 2007;71:313–28.
[16] Karacan CO, Esterhuizen GS, Schatzel SJ, Diamond WP. Reservoir simulation-based modeling for characterizing longwall methane emissions and gob gas venthole production. Int J Coal Geol 2006;71:225–45.
[17] Tonder GJ, Vermeulen PD. The applicability of slug tests in fractured rock formations. Water South Africa 2005;31:157–60.
[18] Lafhaj Z, Shahrour I. Use of water borehole tests for the determination of the permeability of anisotrophic soils. Comp Geotech 2007;34:57–9.
[19] Hawkins JW, Aljoe WW. Pseudokarst groundwater hydrologic characteristics of a mine spoil aquifer. Mine Water Environ 1992;11:37–52.
[20] Maher TP, Donovan JJ. Double-flow behavior observed in well tests of an extremely heterogeneous mine-spoil aquifer. Eng Geol 1997;48: 83–99.
[21] Edmunds WE, Skema VW, Flint NK. Pennsylvanian. Part II: stratigraphy and sedimentary tectonics. In: Geology of Pennsylvania; 1996.
[22] Ferguson HF. Valley stress relief in the Allegheny Plateau. AAPG Bulletin 1967;4:63–8.
[23] Wyrick GG, Borchers JW. Hydrologic effects of stress relief fracturing in an Appalachian valley. US Geological Survey, Water Supply Paper 2177, Washington; 1981.
[24] Stoner J, Williams DR, Buckwalter TF, Felbinger JK, Pattison KL. Water resources and the effects of coal mining, Greene County, Pennsylvania. Water Resource Report 63, Pennsylvania; 1987.
[25] Palchik V. Localization of mining-induced horizontal fractures along rock layer interfaces in overburden: field measurements and prediction. Env Geol 2005;48:68–80.
[26] Faust CR, Mercer JW. Evaluation of slug tests in wells containing a finite-thickness skin. Water Resour Res 1984;20:504–6.
[27] Narasimhan TN, Zhu M. Transient flow of water to a well in an unconfined aquifer: applicability of some conceptual models. Water Resour Res 1993;29:179–91.
[28] Moreno L, Tsang C. Flow channeling in strongly heterogeneous porous media: a numerical study. Water Resour Res 1994;30:1421–30.
[29] Cooper HH, Bredehoeft JD, Papadopulos IS. Response of a finite-diameter well to an instantaneous charge of water. Water Resour Res 1967;3: 263–9.
[30] Bauwer H, Rice RC. A slug test for determining hydraulic conductivity of unconfined aquifers with completely or partially penetrating wells. Water Resour Res 1976;12:423–8.
[31] Dawson KJ, Istok JD. Aquifer testing: design and analysis of pumping and slug tests. Chelsea, Mich: Lewis Pub; 1991.